

## CdS THIN FILMS OBTAINED BY CHEMICAL BATH DEPOSITION IN PRESENCE OF FLUORINE AND THE EFFECT OF ANNEALING ON THEIR PROPERTIES

A. TANUSHEVSKI<sup>a\*</sup>, H. OSMANI<sup>a</sup>

<sup>a</sup>*Institute of Physics, Faculty of Natural Sciences and Mathematics, University "Sts. Cyril and Methodius", 1000 Skopje, Republic of Macedonia*

Thin films of CdS were deposited using chemical bath deposition method (CBD). The effects of thermal treatment on these films in air atmosphere at different temperatures have been studied. As-prepared and annealed films were polycrystalline with hexagonal structure. The structural properties of the CdS films, the average diameter of the grains ( $D$ ) and the dislocation density ( $\delta$ ) were determined by means of X-ray diffraction. AFM image analysis showed that the films annealed at temperature of 400 °C have the largest grain size. The optical absorption measurements showed that the direct band gap of the films and Urbach energy values of the films are changing with the annealing process. Additionally, the band gap of the films was determined by the photoconductivity spectra, showing similar values as optical band gap determined by parabolic approximation. The fast photoconductivity varies by changing the heat-treatment conditions and the maximum photoconductivity was found for films annealed at temperature of 450 °C.

(Received November 8, 2017; Accepted February 11, 2018)

*Keywords:* Chemical bath deposition, CdS thin films, Effect of annealing, Electrical properties.

### 1. Introduction

CdS is an n-type II-VI compound with a direct band gap of 2.42 eV, and is suitable for use in solar cells. It is also applied in some photosensor devices, light-emitting diode, FET transistor, photocatalytic device and optoelectronic device [1, 2]. In addition, the CdS thin film can be nanocrystalline, allowing for its wider use in electronic and optical devices [2]. However, CdS is used for production of cheap and efficient solar cells type CdS/CdTe and CdS/CuInSe<sub>2</sub> [3]. In these heterolayered solar cells, CdS acts as a window semiconductor and partner in the production of a heterolayered solar cell [1, 4].

The CBD method is suitable for obtaining thin films with large surface area, with the possibility to change the size of the grains depending on the solution conditions [4]. Also, the method is cheap and suitable for photovoltaic applications. To obtain a CdS thin film an alkaline solution is usually used where NH<sub>4</sub>OH serves as complexing reagent of Cd<sup>2+</sup> ions and at the same time depending on its amount the solution pH value changes. The use of complex cadmium salt allows slow release of Cd<sup>2+</sup> ions, and thereby increasing the probability for their interaction by sulfur ions S<sup>2-</sup> [2], [5, 6]. Several methods are used for the deposition of a CdS thin film, such as chemical bath deposition [1] [3, 6], photochemical deposition [7], electrochemical deposition [8], thermal vacuum evaporation [9], RF magnetron sputtering [10], close space sublimation [11], and spray pyrolysis [12].

---

\*Corresponding author: atanas@pmf.ukim.mk

## 2. Experimental

The CdS thin films were deposited on glass substrate using CBD technique. The substrates used for the deposition were commercial glass slides of 76 mm × 25 mm. Before the deposition occurred, the glass substrates were carefully cleaned by chromic acid for 60 min and then finally washed with deionised water. In the chemical bath deposition procedure, the substrate was immersed in an aqueous bath containing 20 ml of 0.1 M CdCl<sub>2</sub>, 5 ml of 1 M NH<sub>4</sub>F, 4 ml of 1 M thiourea and NH<sub>3</sub>. In the presence of NH<sub>3</sub> as a complexing agent, the pH of the aqueous solution was 10. For the present work, the use of ammonium fluoride [12] served as a stabilizing buffer agent and it has been proved that fluorine is not an effective dopant in CdS, since no change in the resistivity of the CdS layers was observed [13]. As-grown films were deposited at temperature of  $T = 90\text{ }^{\circ}\text{C}$ , within deposition time of 5 min ( $t_d$ ), which resulted in 0.15  $\mu\text{m}$  thickness of the films. Additionally, they were subject to further investigation. The obtained CdS films were homogeneous and well adhered to the substrate. In order to increase the film crystallinity, they were rapidly annealed in air at various temperature of 200  $^{\circ}\text{C}$ , 250  $^{\circ}\text{C}$ , 300  $^{\circ}\text{C}$ , 400  $^{\circ}\text{C}$  and 450  $^{\circ}\text{C}$ , and further on, used in this research.

The crystal structure of the films was studied using X-ray diffraction (XRD) measurements obtained with a Rigaku Ultima IV powder X-ray diffractometer, for  $2\theta$  in range 20 $^{\circ}$ -70 $^{\circ}$ . As a radiation source we used Cu-K $_{\alpha}$  radiation with  $\lambda = 0.15418\text{ nm}$ , obtained from a generator set at 40 kV and a current of 40 mA, with a scan rate of 2  $^{\circ}/\text{min}$ . The AFM images of the surfaces of the films were taken with a Scanning Probe Microscope SPM-9700 operating in dynamic mode. The optical transmission spectra of the deposited thin films of CdS was determined with a Varian Cary 50 spectrophotometer in order to determine the band gap energy, within the range of 300-900 nm.

Electrical measurements were made with the constant field method, whereby the CdS thin film was connected in a series with a standard resistor and d. c. voltage source [14]. The photoconductivity spectra of the of CdS films was found in the range of 480–570 nm by using a Deuterium lamp of the spectrophotometer Beckman DU-2, previously calibrated to the incident photon flux. In addition, the fast photoconductivity was measured as a function of time using a HEWLETT PACKARD 54600B 100 MHz digital storage oscilloscope, where the sample was illuminated by flash light.

## 3. Results and discussion

Fig. 1 shows XRD patterns of CdS thin films, as-grown and air annealed at different temperatures of 200  $^{\circ}\text{C}$ , 250  $^{\circ}\text{C}$ , 300  $^{\circ}\text{C}$ , 400  $^{\circ}\text{C}$  and 450  $^{\circ}\text{C}$ . The curves show that the CdS films have a pronounced peak at 26.51 $^{\circ}$ , which corresponds to preferred orientation of the crystals along the plane (002). Other peaks were found at 24.81 $^{\circ}$ , 28.18 $^{\circ}$ , 43.69 $^{\circ}$  and 51.82 $^{\circ}$ , corresponding to planes (100), (101), (110) and (112), respectively. The data obtained from the XRD images and their comparison with the diffraction images of the reference card JPDS 41-1049 indicate that the as-grown and annealed at different temperatures of 200  $^{\circ}\text{C}$ , 250  $^{\circ}\text{C}$ , 300  $^{\circ}\text{C}$ , 400  $^{\circ}\text{C}$  and 450  $^{\circ}\text{C}$  have hexagonal (wurtzite) crystal structure [15]. The thermal treatment at 400  $^{\circ}\text{C}$  contributes to growth of the peak of the plane (002), but after thermal treatment at 450  $^{\circ}\text{C}$  the peak corresponding to the plane (002) decreases. On the other hand, there is the appearance of other peaks corresponding to the hexagonal crystalline structure, however a peak corresponding to the CdO compound also appears (Fig. 1).

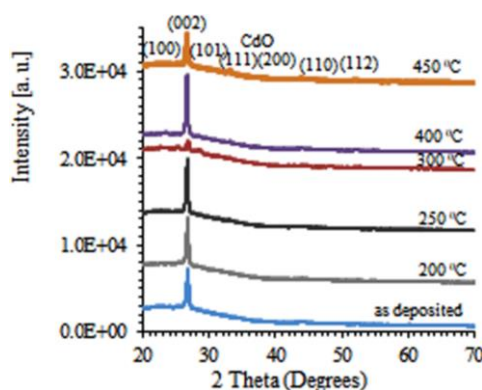


*Fig. 1. XRD patterns obtained from as-grown and annealed CdS thin films at different temperatures*

The XRD patterns provide an opportunity to determine the structural properties of the CdS films such as the size of the grains  $D$ . Usually, the highest peak of XRD patterns is a major characteristic of the films, so that the average grain size is calculated using the Debye-Scherrer relation [16]. Table 1 shows the values of the grain size of the CdS films from the substrate temperature. It is obvious that the grain size increases with the rise of temperature, until the temperature reaches a value of 250 °C. However, annealing the substrates at a temperature of 300 °C contributes to a sharp decline in the height of the peak relating to the plane (002) and the appearance of other adjacent peaks in the XRD images. This indicates crystallization of film impurities, leading to segregation in films and reducing the grain size. While the grains become larger and increase in size with film annealing at 400 °C. Further increase in temperature to 450 °C contributes to reducing the size of the grains again. The recrystallization of the grains leads to creation of induced defects in the film structure [3].

For better characterization of CdS thin films, their structural parameters were determined in order to predict their impact on the optical and photoelectric properties. Although the density of dislocations ( $\delta$ ) decreases as the annealing temperature increases, it has great value for the as-grown films and annealed films at temperature of 300 °C (table 1). The lowest value of the density of dislocations ( $\delta$ ) is obtained at annealing temperature of 400 °C. The defects appearing in the CdS films depend on the annealing temperature and may occur as impurity levels in the band gap or be recombination centers.

The morphology of films was determined by AFM (atomic force microscopy), whereby the film surface studied was 1  $\mu\text{m}$  x 1  $\mu\text{m}$  (figure 2). The size of the grains determined by AFM images is consistent with the results obtained from XRD measurements. As-grown films (figure 2a) represent clusters with globular form whereby the size of the grains is about 23 nm and is in line with the calculations made from the XRD images. Film annealing at a temperature of 200 °C and 250 °C contributes to the increase of growth of the grains in the clusters (figure 2b and figure 2c). On the other hand, film annealing at a temperature of 300 °C contributes to the segregation of the films and decrease of the grain size (figure 2d). The impurities in the clusters were crystallized, resulting in their bursting and decreasing of their grain size. Annealing of the films at a temperature of 400 °C contributes to transformation of the clusters into grains which have sharp edges (figure 2e). Therefore, the films annealed at temperatures of 400 °C showed the highest peak observed in the XRD patterns. Although the grain size of the films annealed at temperature of 450 °C had been increased, small cavities appeared on the surface of the films caused by oxidation process of the films (fig. 1 and fig. 2f).

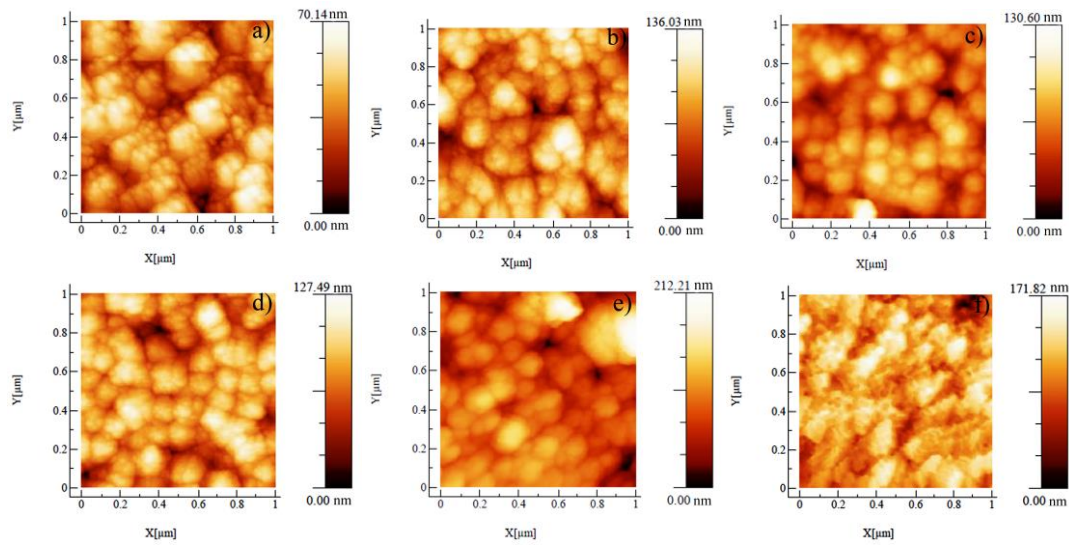


Fig. 2. AFM images of the surface of CdS films: a) as-grown, b) annealed at temperature 200 °C, c) annealed at temperature 250 °C, d) annealed at temperature 300 °C, e) annealed at temperature 400 °C and f) annealed at temperature 450 °C

The transmission spectra of as-grown and air-annealed CdS thin films at different temperatures are shown in Fig. 3. As-grown thin films of CdS show a significant increase of transmission, corresponding to a wavelength of 500 nm. It is evident that the measured transmission in dependence on the wavelength for films treated at temperature of 300 °C, show a gradual incline in the curve, due to smaller grain size, amorphous phase in the films and segregation of impurities of the grains.

The absorption coefficient of the films was calculated from the transmittance spectra by the relation [9]:

$$\alpha = \frac{1}{d} \ln\left(\frac{1}{T}\right) \quad (1)$$

where  $T$  is the transmittance and  $d$  is the thickness of the film. The curves obtained as result of the absorption coefficient in dependence on the photon energy are shown in figure 4. In the photon energy region from 2.2 eV to 2.5 eV, the energy dependence of the absorption coefficient ( $\alpha = 10^4$ - $10^5 \text{ cm}^{-1}$ ) suggests the occurrence of direct electron transitions. Furthermore, the absorption coefficient of CdS films grows linearly with the photon energy in the range from 2.20 - 2.60 eV, which indicates on a strong light absorption in the films.

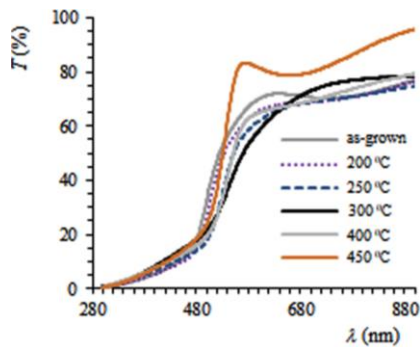


Fig. 3. Transmission spectra of the CdS thin films as a function to the substrate temperature

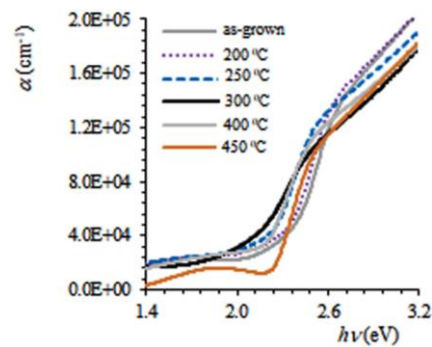


Fig. 4. Dependence of absorption coefficient versus photon energy, and as a function to the substrate temperature

On the other hand, we have a linear dependency of the absorption coefficient on the photon energy, where the small inclination of the curve may suggest presence of amorphous structure and weak crystallization of the film. Therefore, the Urbach energy can be determined from the exponential value of the absorption coefficient of the photon energy [17]. In fact, the Urbach energy value ( $E_U$ ) is calculated from the reciprocal value of the coefficient in the direction of the curve obtained from a graphical presentation of  $\ln(\alpha)$  from the photon energy (figure 5), and the same is given in table 1. The values of  $E_U$  energy decrease up to temperature of 250 °C, then increase at temperature of 300 °C and again decrease for temperatures higher than 400 °C. The annealing of films at temperature of 450 °C contributes for obtaining the smallest value of Urbach energy, and thus, defined crystal structure of films.

The optical band gap  $E_g$  of the films can be determined by using a graphic presentation of  $(\alpha h\nu)^2 = f(h\nu)$  and from the intersection of the straight part of the curves with the x-axis (figure 6). From figure 6, it is evident that the direct band gap of the samples decreases from 2.38 eV to 2.20 eV to the temperature of 300 °C (table 1), while it increases by increasing the temperature from 400 °C to 450 °C.

The light absorption in the semiconductor makes electrons from the valence band jump up in the conduction band, at the same time increasing the film conductivity. Therefore, the largest photoconductivity of CdS films should come from photons with energy of 2.4 eV [18]. For this reason, when it comes to the intrinsic photoconductivity of the film, the optical band gap should be determined from the maximum photoconductivity [19]. Also, the energy band gap of the CdS thin films was determined from the measurement of the spectral response of photoconductivity  $\sigma_{ph}$ , normalized (calibrated) to the photon flux and the obtained value was compared to the optical band gap (table 1). Namely, in the low-photon-energy range ( $ad < 1$ ), photoconductivity  $\sigma_{ph}$  is proportional to  $\alpha$  and therefore it can be used for determining the band gap energy [20]. The energy band gap was measured from the red boundary of curves  $(\sigma h\nu)^2 = f(h\nu)$ , i.e. the intersection of the straight part of the curves with the x-axis (figure 7). The band gap determined on this way is close to a band gap determined by parabolic approximation (table 1). On the other hand, for photon energy higher than 2.5 eV, the photoconductivity decreases and in the range of 2.5 eV to 3 eV ( $ad > 1$ ), the photoconductivity  $\sigma_{ph}$  is not proportional to  $\alpha$ .

The fast photoconductivity is important since the shape of the curve can determine the relaxation time and the carrier recombination type. Namely, the nature of traps and the recombination centers in the semiconductor [21] can be determined from the rising and falling curve. The fast photoconductivity of CdS thin films as-grown and annealed at temperature of 200 °C, 250 °C, 250 °C, 300 °C, 400 °C and 450 °C are shown on figure 8. The film treated at temperature of 450 °C showed highest rate of photoconductivity, and furthermore, the lowest rate of photoconductivity was attributed to the temperature of 300 °C.

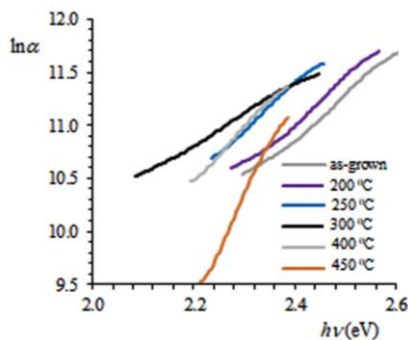


Fig. 5 Variation of  $\ln\alpha$  versus  $h\nu$  for samples of the CdS thin films as a function to the substrate temperature.

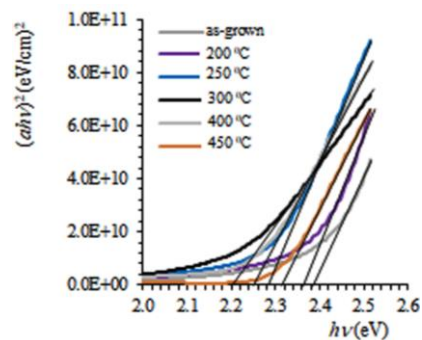


Fig. 6 The dependence of  $(\alpha h\nu)^2$  on the photon energy ( $h\nu$ ) of the CdS thin films at different substrate temperature for direct allowed transitions.

Table 1. Structural parameters, energy band gap and Urbach energy of CdS thin films.

$T$ (°C)	$D$ (nm)	$\square$ $\times 10^{15}$ ( $\text{lin}/\text{m}^2$ )	$E_{g(\text{op})}$ (eV)	$E_{g(\text{ph})}$ (eV)	$E_u$ (eV)
as-grown	23	1.94	2.38	2.37	0.253
200	27	1.35	2.36	2.32	0.245
250	30	1.09	2.28	2.29	0.230
300	23	1.94	2.20	2.27	0.351
400	30	1.09	2.25	2.28	0.198
450	27	1.35	2.31	2.31	0.102

The films that were annealed at 300 °C have high Urbach energy value (table 1), which indicates on present structural defects that might be centers of recombination of photogenerated carriers [20].

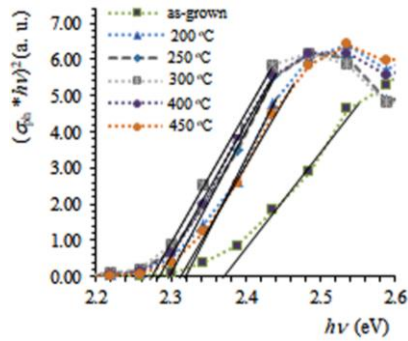


Fig. 7. The dependence of  $(\sigma_{ph} * hv)^2$  on the photon ( $h\nu$ ) of the CdS thin films annealing at different temperatures.

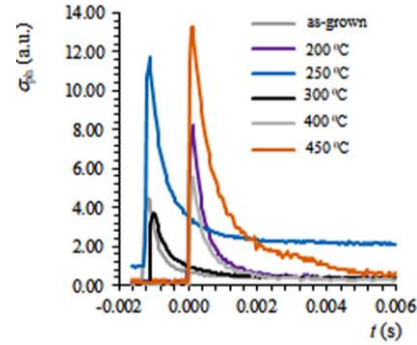


Fig. 8. Photoconductive decay of CdS thin films as a function of substrate temperature.

#### 4. Conclusions

CdS thin films were deposited on glass substrates with chemical bath deposition (CBD) of water solution of cadmium chloride, thiourea, and buffer solution of cadmium fluoride, for five minutes. The film structure was determined from XRD patterns which demonstrated that the as-grown and air annealed films have wurtzite crystal structure. The grain size increases at 400 °C, which leads to coalescence between clusters and formation of grains. However, the films annealed at temperature of 450 °C oxidize partially and their grain size decreases. Grain form and size was determined from the AFM images, which are in accordance with the results obtained from XRD patterns.

At temperature of 300 °C the Urbach energy has highest value, which seems to be due to the crystallization of the impurities in the films. The smallest value of Urbach energy is obtained for CdS films annealed at 450 °C, at which temperature they should have the best crystal structure.

The optical band gap of the films decreases from 2.38 eV to 2.20 eV as the temperature increases to 300 °C, and then it increases again to 2.31 eV as the temperature increases to 450 °C. The band gap determined by the normalized photoconductivity spectra of CdS thin films as a function of photon energy, at different temperatures is close to band gap determined by parabolic approximation. The fast photoconductivity of CdS thin films showed maximum value at temperature of 450 °C, and minimum value at temperature of 300 °C. The small cavities that were created during the annealing of films at 450 °C will increase the light absorption, at the same time

increasing the photoconductivity of films. It is obvious that the fast photoconductivity is in correlation with Urbach energy of the films.

### Acknowledgment

The authors would like to express their sincere gratitude to the Faculty of Natural and Technical Sciences at the "Goce Delchev" University of Shtip, for the AFM measurements.

### References

- [1] H. Metin, R. Esen, *Journal of Crystal Growth*, **258**(1), 141 (2003).
- [2] H. Khallaf, I. O. Oladeji, G. Chai, L. Chow, *Thin Solid Films*, **516**(21), 7306 (2008).
- [3] A. Kariper, E. Guneri, F. Gode, C. Gumus, T. Ozpazan, *Materials Chemistry and Physics* **129**, 183 (2011).
- [4] A. E. Abken, D. P. Halliday, and K. Durose, *J. Appl. Phys.*, **105**, 064515 (2009).
- [5] M. B. Ortuño López, J.J. Valenzuela-Jáuregui, M. Sotelo-Lerma, A. Mendoza-Galván, R. Ramírez-Bon, *Thin Solid Films*, **429**(1), 34 (2003).
- [6] J. M. Dofia and J. Herrero, *J. Electrochem. Soc.*, **144**(11), 4081 (1997).
- [7] M. Ichimura, F. Goto and E. Arai, *J. Appl. Phys.*, **85**, 7411 (1999).
- [8] R. P. Raffelle, H. Forsell, T. Potdevin, R. Friedfeld, J.G. Mantovani, S.G. Bailey, S.M. Hubbard, E.M. Gordon, A.F. Hepp, *Solar Energy Materials & Solar Cells* **57**, 167 (1999).
- [9] S. A.-J. Jassim, A. A. R. A. Zumaila, G. A. A. A. Waly, *Results in Physics*, **3**, 173 (2013).
- [10] A. Rios-Flores, O. Arés, J. M. Camacho, V. Rejon, J.L. Peña, *Solar Energy*, **86**, 780 (2012).
- [11] J. P. Enríquez, X. Matthew, G.P. Hernández, U. Pal, C. Magaña, D.R. Acosta, R. Guardian, J.A. Toledo, G. C. Puentef, J.A. C. Carvayar, *Solar Energy Materials & Solar Cells* **82**(1), 307 (2004).
- [12] J. Santos Cruz, R. Castanedo Pérez, G. Torres Delgado, O. Zelaya Angel, *Thin Solid Films*, **518**(7), 1791 (2010).
- [13] Salih Yılmaz, *Applied Surface Science*, 357 (2015) 873.
- [14] С.М. Рывкин, *Фотоэлектрические явления в полупроводниках.*, Гос. Изд. Физ. Мат. Лит., Москва, 37 (1963).
- [15] R. Ramírez-Bon, N C Sandoval-Inday, F J Espinoza- Beltrán, M Sotelo-Lerma, O. Zelaya-Angel and C Falcony, *J. Phys.: Condens. Matter*, **9**(45), 10051 (1997).
- [16] A. Cortes, H. Gómez, R.E. Marotti, G. Riveros, E.A. Dalchiel, *Solar Energy Materials & Solar Cells*, **82**(1), 21 (2004).
- [17] A.S. Hassanien, A. A. Akl, *Superlattices and Microstructures*, **89**, 153 (2016).
- [18] S. L. Sheng, *Semiconductor Physical Electronics* 2nd ed., Springer Science+Business Media, 264(2006).
- [19] O. Vigil, I. Riech, M. Garcia-Rocha and O. Zelaya-Angel, *J. Vac. Sci. Technol. A* **15**, 2282 (1997).
- [20] A. E. Rakhshani and A. S. Al-Azab, *J. Phys.: Condens. Matter*, **12**(40), 8745 (2000).
- [21] H. Moualkia, S Hariech, M S Aida, N Attaf and E L Laifa, *J. Phys. D: Appl. Phys.* **42**(13), 135404 (2009).